

Electronic Supporting Information

Interlayer Bonding Strength of 3D Printed PEEK Specimens

Chya-Yan Liaw¹, John W. Tolbert³, Lesley W. Chow^{4,5} and Murat Guvendiren^{1,2,*}

¹ Otto H. York Department of Chemical and Materials Engineering, New Jersey Institute of Technology, Newark, NJ, 07102, USA

² Department of Biomedical Engineering, New Jersey Institute of Technology, Newark, NJ, 07102, USA

³ Department of Materials Science and Engineering, Lehigh University, Bethlehem, PA 18015, USA

⁴ Department of Bioengineering, Lehigh University, Bethlehem, PA 18015, USA

***Corresponding Author**

Dr. Murat Guvendiren

Otto H. York Department of Chemical and Materials Engineering

New Jersey Institute of Technology

161 Warren Street, 150 Tiernan Hall

Newark, NJ 07102 USA

Phone: 973-596-2932

Fax: 973-596-8436

e-mail: muratg@njit.edu

Supplemental Figures

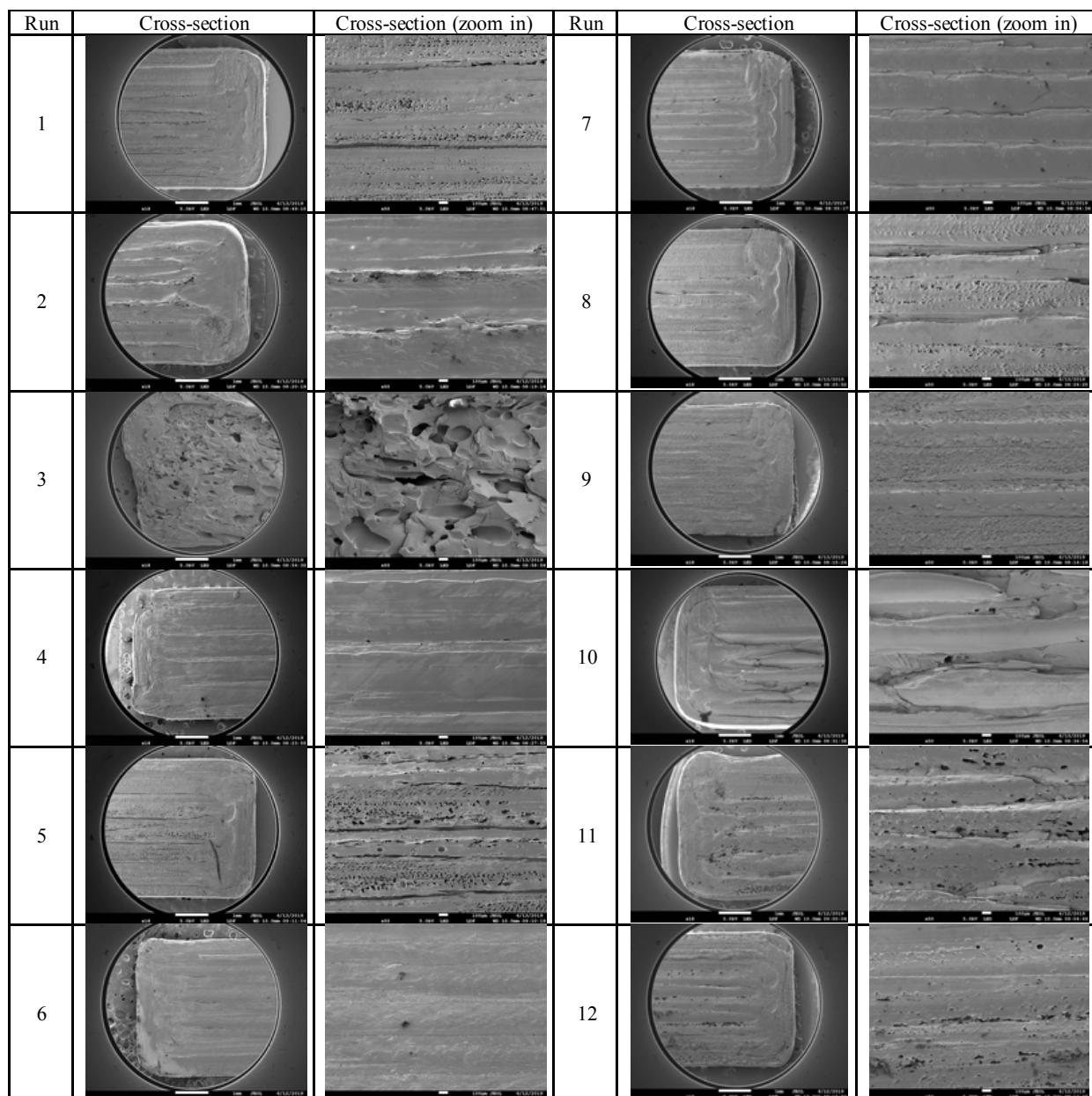


Figure S1. Cross-sectional SEM images of the fractured surfaces.

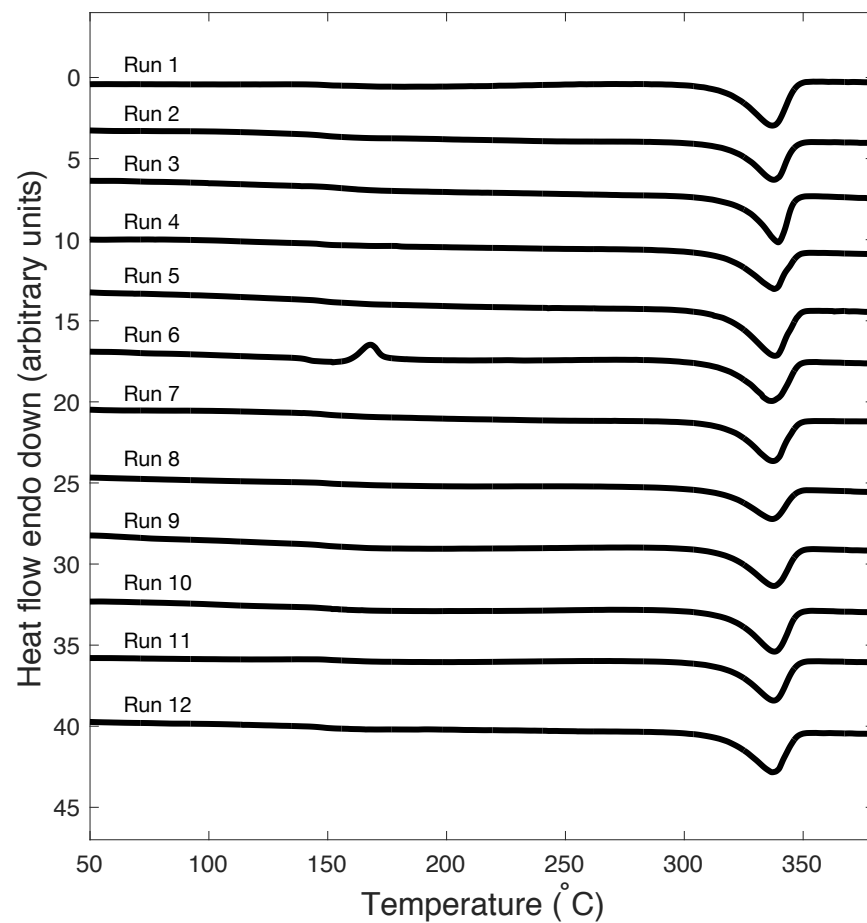


Figure S2. DSC curves for the 3D-printed PEEK samples obtained at different experimental settings (*Runs*) including nozzle temperature, print speed, layer height, and wait time. Refer to Table 3 in the manuscript for the setting for each *Run*.

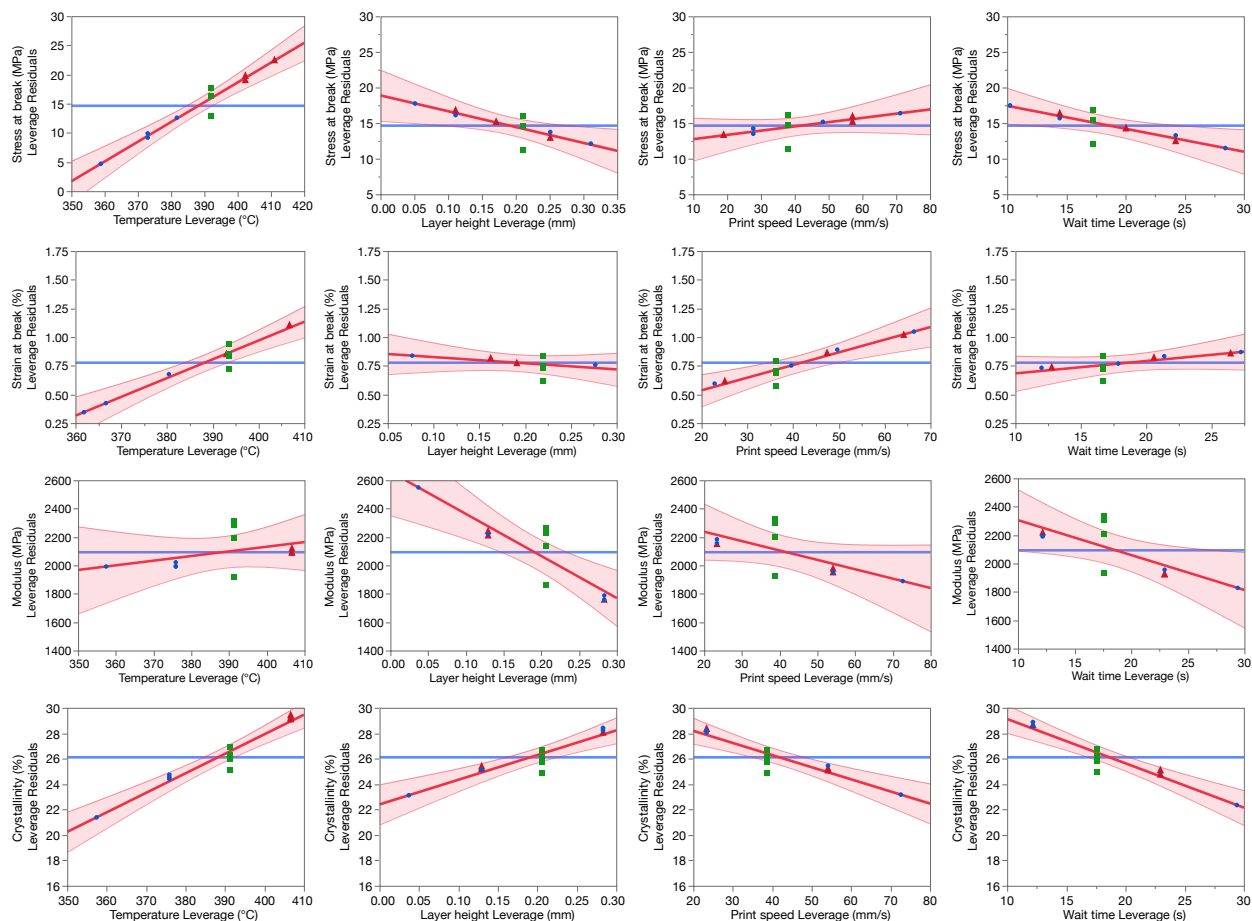


Figure S3. Leverage residual plots of the factors (temperature, layer height, print speed, and wait-time) for each response (stress, strain, modulus, and crystallinity). Each row represents a response, and each column represents a factor. Leverage residual plots are used to visualize the influential data points on the model and to identify the significant factors. The blue line depicts the average of the leverage residuals. The red line shows the fitting by the model, with light red regions showing the confidence intervals. The slope of the red line indicates the degree and direction of factor influence on the response. The blue circles, green squares, and red triangles represent the conditions printed at temperatures at the low, center, and high settings, respectively.

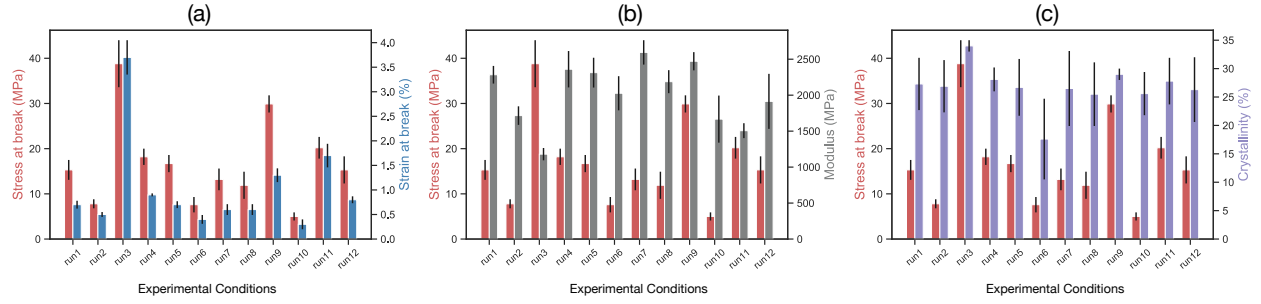


Figure S4. Stress at break and strain at break (a), stress at break and modulus (b), and stress at break and crystallinity (c), measured in 12 different conditions (*Runs*).

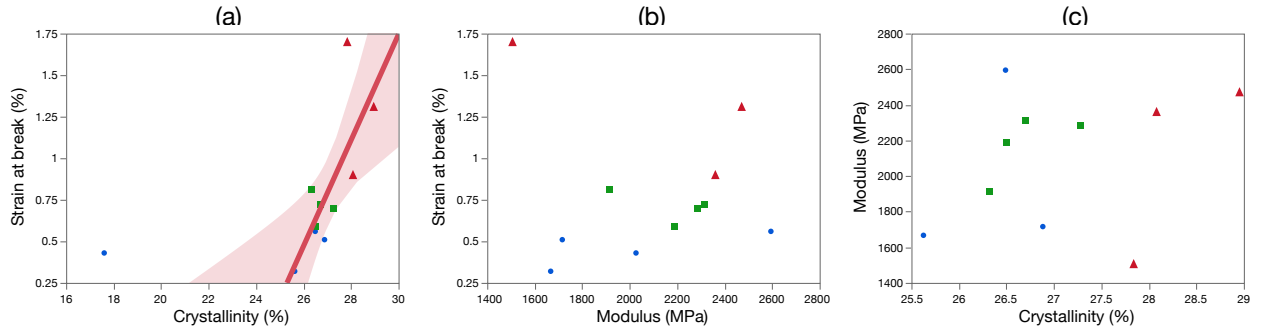


Figure S5. A positive correlation was found between (a) strain at break and crystallinity (Strain at break = $-7.8 + 0.32 \cdot \text{Crystallinity}$, $p = 0.0103$). But no correlation was found between (b) strain at break and modulus, and (c) modulus and crystallinity.

Supplementary Tables

Table S1. Experimental design matrix developed by JMP's DOE platform, the corresponding results (responses), the rheological results, and the calculated values

Run	Process Parameters (Factors)				Measurements (Responses)				Rheological results and Calculated Values			
	T (°C)	PS (mm/s)	LH (mm)	WT (s)	Stress at break (MPa)	Strain at break (%)	Modulus (MPa)	Crystalline (%)	Flow rate (mm ³ /s)	Shear rate (s ⁻¹)	Apparent Viscosity (Pa·s)	Contact pressure (MPa)
1	390	40	0.2	18	15.3 ± 2.2	0.7 ± 0.08	2284.0 ± 122.6	27.3 ± 4.6	2.1	330	610	2.4
2	370	60	0.3	11	7.8 ± 1.0	0.5 ± 0.05	1716.1 ± 128.9	26.9 ± 4.6	4.8	760	520	1.4
3	410	20	0.3	11	36.4 ± 5.2	3.7 ± 0.35	1180.0 ± 85.7	34.0 ± 1.0	1.6	250	520	0.5
4	410	20	0.1	25	18.2 ± 1.8	0.9 ± 0.03	2360.7 ± 252.9	28.1 ± 2.1	0.5	80	800	6.0
5	390	40	0.2	18	16.7 ± 1.9	0.7 ± 0.07	2313.3 ± 207.1	26.7 ± 5.0	2.1	330	610	2.4
6	370	60	0.1	25	7.6 ± 1.7	0.4 ± 0.09	2026.6 ± 237.3	17.6 ± 7.1	1.6	250	808	19.4
7	370	20	0.1	11	13.2 ± 2.4	0.6 ± 0.11	2594.7 ± 169.5	26.5 ± 6.6	0.5	80	1210	9.1
8	390	40	0.2	18	11.9 ± 3.0	0.6 ± 0.11	2187.7 ± 160.0	25.5 ± 5.6	2.1	330	610	2.4
9	410	60	0.1	11	29.9 ± 1.9	1.3 ± 0.14	2471.6 ± 126.6	29.0 ± 1.0	1.6	250	520	12.5
10	370	20	0.3	25	5.0 ± 0.9	0.3 ± 0.10	1667.2 ± 327.3	25.6 ± 3.8	1.6	250	808	0.7
11	410	60	0.3	25	20.2 ± 2.4	1.7 ± 0.24	1506.5 ± 103.6	27.8 ± 4.1	4.8	760	330	0.9
12	390	40	0.2	18	15.3 ± 3.0	0.8 ± 0.07	1914.1 ± 382.4	26.3 ± 5.7	2.1	330	610	2.4

Table S2. The identified important parameters and the estimated coefficients in the models for flexure stress at break, strain at break, modulus and crystallinity. p-values mark with * denote the factor being significant. The parameters are sorted in decreasing order of significance. Note that the parameter estimates are calculated in terms of the coded values of each factor (from -1 to 1).

Stress at break (MPa)					Strain at break (%)				
Term	Coefficient	Std Error	t-ratio	p-value	Term	Coefficient	Std Error	t-ratio	p-value
T	6.67	0.59	11.35	<0.0001*	T	0.31	0.04	7.95	0.0005*
WT	-2.33	0.59	-3.97	0.0107*	PS	0.22	0.04	5.52	0.0027*
LH	-2.14	0.59	-3.66	0.0146*	T* PS	0.20	0.04	5.14	0.0036*
T*PS	2.01	0.59	3.42	0.0188*	T*WT	0.15	0.04	3.75	0.0133*
PS	1.31	0.59	2.23	0.0764	WT	0.07	0.04	1.73	0.1450

Modulus (MPa)					Crystallinity (%)				
Term	Coefficient	Std Error	t-ratio	p-value	Term	Coefficient	Std Error	t-ratio	p-value
LH	-357.34	78.39	-4.56	0.0014*	T	3.10	0.20	15.30	<0.0001*
					WT	-2.46	0.20	-12.16	<0.0001*
					LH	1.97	0.20	9.72	<0.0001*
					PS	-1.93	0.20	-9.53	<0.0001*

Table S3. Shift factors and zero-shear viscosity values.

Temperature (°C)	Horizontal shift factor a_T	Zero-Shear Viscosity (Pa·s)
345	7.36596	16872.60
350	1.23225	5564.56
360	1.04788	4231.62
370	1.00000	4114.34
380	0.91830	3093.92
390	0.76669	3068.58
400	0.63526	2431.76
410	0.46897	2009.02

Note that the zero-shear viscosity was obtained by fitting the flow curves with the Williamson model.
The R^2 is over 0.99 for all fittings.

Regression Model Evaluation

To assess the relationship between the 3D printing process parameters (nozzle temperature, print speed, layer height, and wait-time) and the responses (flexural stress at break, strain at break, modulus, and crystallinity), a linear regression model was developed by fitting the data using a least square method. The general linear regression model (for a resolution IV design) is shown below:

$$\begin{aligned} y = & (\alpha_0 + \alpha_{1234}) + (\alpha_1 + \alpha_{234})x_1 + (\alpha_2 + \alpha_{134})x_2 + (\alpha_3 + \alpha_{124})x_3 + (\alpha_4 + \alpha_{123})x_4 \\ & + (\alpha_{12} + \alpha_{34})(x_1x_2 \text{ or } x_3x_4) + (\alpha_{13} + \alpha_{24})(x_1x_3 \text{ or } x_2x_4) \\ & + (\alpha_{14} + \alpha_{23})(x_1x_4 \text{ or } x_2x_3) + \varepsilon \end{aligned}$$

where y is the response; x_i ($i = 1, 2, 3, 4$) are the main process parameters (or factors); α_i are the coefficients associated with the main factors; α with two- three- and four-digits subscript are the coefficients associated with two-factor, three-factor and four-factor interactions respectively; α_0 is the intercept; and ε is the random error term. In practice, the higher-order effects (three-factor interactions and more) are considered less important and can be neglected. Therefore, the model for a resolution IV design enables estimation of the main effects.

The fitted results for all responses, including the coefficients are summarized in **Table S3**. The t-ratio is the ratio of the coefficient to the standard error (Std Error), and is used to determine the p-value. The p-value can be used to test if the coefficient of the processing parameter is significantly different from zero or not. The smaller the p-value (typically ≤ 0.05), the higher the significance of the process parameter.

Several key areas of model evaluation include: summary of fit, actual-by-predicted plot, analysis of variance, lack-of-fit test, and the residual analysis.

Modelling Stress at Break

Predictive model

$$\begin{aligned} \hat{Y}_{stress} = & 15.16 + 6.67 \times \left(\frac{T - 390}{20} \right) + 1.31 \times \left(\frac{PS - 40}{20} \right) - 2.15 \times \left(\frac{LH - 0.2}{0.1} \right) \\ & - 2.33 \times \left(\frac{WT - 18}{7} \right) + 2.01 \times \left(\frac{T - 390}{20} \right) \times \left(\frac{PS - 40}{20} \right) \end{aligned}$$

Note that JMP uses -1 and $+1$ coding for the analysis, not the real physical unit. Therefore, one unit change corresponds to the change from low level of setting to the midpoint or the midpoint to the high level of setting. The interpretation of the equation is as follows: for every unit increase in temperature (from 370°C to 390°C or from 390°C to 410°C), the stress at break will increase by 6.67 times when all other factors are held constant; for every unit increase in wait-time (from 11s to 18s or from 18s to 25s), the stress at break will decrease by 2.33 times when all other factors are held constant; for every unit increase in layer height (from 0.1 mm to 0.2 mm or from 0.2 mm to 0.3 mm), the stress at break will decrease by 2.15 times when all other factors are held constant.

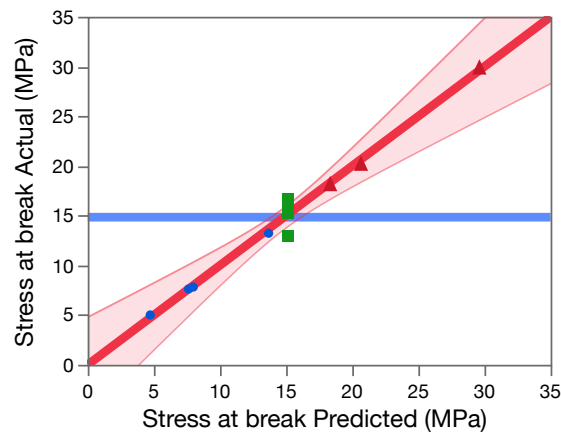
Summary of fit

The adjusted R-square is high, showing that around 96% of the variability in stress at break was explained by the model.

R-Square	Adjusted R-Square	Root Mean Square Error	Mean of Response
0.98	0.96	1.389	14.843

Actual by Predicted Plot

From the Actual by Predicted plot, the confidence band (pink region) does not completely include the blue line, and the p-value is 0.0003 (less than 0.05), indicating that the overall model is significant. The data points colored red, green, and blue corresponds to the results obtained at the highest, medium, and lowest temperature setting.



Analysis of Variance

The overall model p value is smaller than 0.05, suggesting that at least one of the parameters is significantly different from 0.

Source	df	Sum of square	Mean Square	F-Ratio	Prob > F
Regression	5	467.692	93.538	48.486	0.0003
Residual	5	9.646	1.929		
Total	10	477.338			

Lack of Fit

Because of the 4 replicated center points, JMP was able to perform the Lack of Fit test. The Lack of Fit test is to test if the error in the prediction is due to lack of model fit.

H_0 (null hypothesis): There is no lack of fit

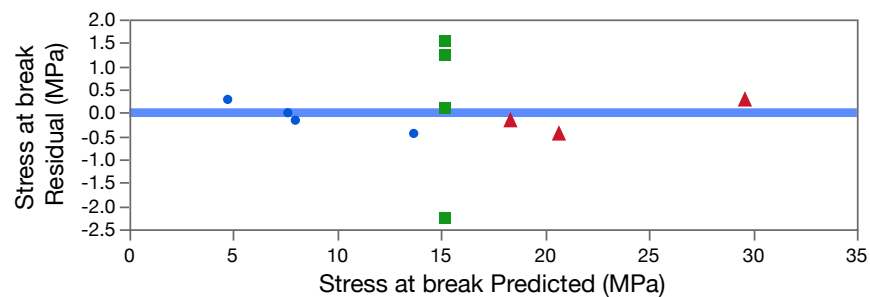
H_a (alternative hypothesis): There is lack of fit

Since the p-value for the lack of fit test is 0.891 (greater than 0.05), there is not enough evidence at a 0.05 level to conclude that there is a lack of fit.

Source	df	Sum of square	Mean Square	F-Ratio	Prob > F
Lack of fit	2	0.715	0.358	0.12	0.891
Pure error	3	8.931	2.977		
Total error	5	9.646			

Residual by Predicted Plot and Normality of Residuals

There is no clear pattern found in the Residual by Predicted plot, and the residuals are centered around zero through the range of predicted values. In addition, the p-value for the Anderson Darling normality test is greater than the alpha level of 0.05. Therefore, there is insufficient evidence to reject the null hypothesis that the residuals of the stress at break are normally distributed.



Anderson-Darling	
A2	Prob > A2
0.587	0.107

Modelling Strain at Break

Predictive model

For every unit increase in temperature (from 370°C to 390°C or from 390°C to 410°C), the strain at break will increase by 0.31 times when all other factors are held constant; for every unit increase in print speed (from 20 mm/s to 40 mm/s or from 40 mm/s to 60 mm/s), the strain at break will increase by 0.22 times when all other factors are held constant.

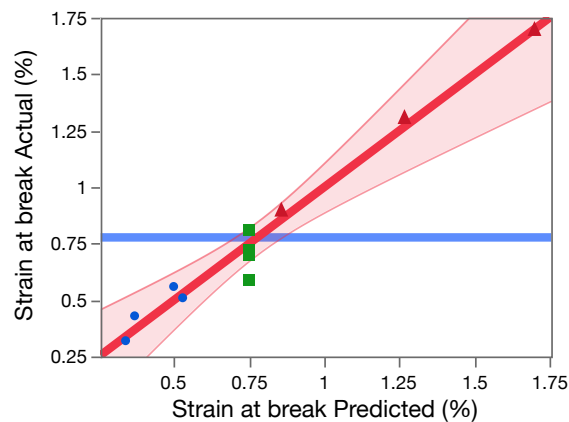
$$\hat{Y}_{strain} = 0.75 + 0.31 \times \left(\frac{T - 390}{20}\right) + 0.22 \times \left(\frac{PS - 40}{20}\right) + 0.07 \times \left(\frac{WT - 18}{7}\right) \\ + 0.2 \times \left(\frac{T - 390}{20}\right) \times \left(\frac{PS - 40}{20}\right) + 0.15 \times \left(\frac{T - 390}{20}\right) \times \left(\frac{WT - 18}{7}\right)$$

Summary of Fit

The adjusted R-Square is relatively low due to the leverage point.

R-Square	Adjusted R-Square	Root Mean Square Error	Mean of Response
0.973	0.947	0.094	0.777

Actual by Predicted Plot



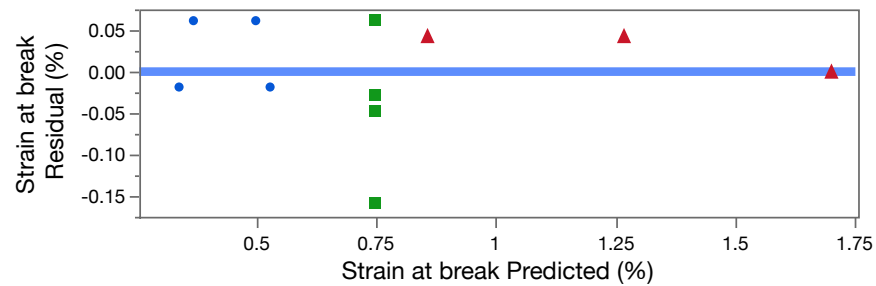
Analysis of Variance

Source	df	Sum of square	Mean Square	F-Ratio	Prob > F
Regression	5	1.6	0.32	36.571	0.0006
Residual	5	0.044	0.009		
Total	10	1.644			

Lack of Fit

Source	df	Sum of square	Mean Square	F-Ratio	Prob > F
Lack of fit	2	0.019	0.01	1.179	0.419
Pure error	3	0.025	0.008		
Total error	5	0.044			

Residual by Predicted Plot and Normality of Residuals



Anderson-Darling	
A2	Prob > A2
0.6	0.08

Modelling Modulus

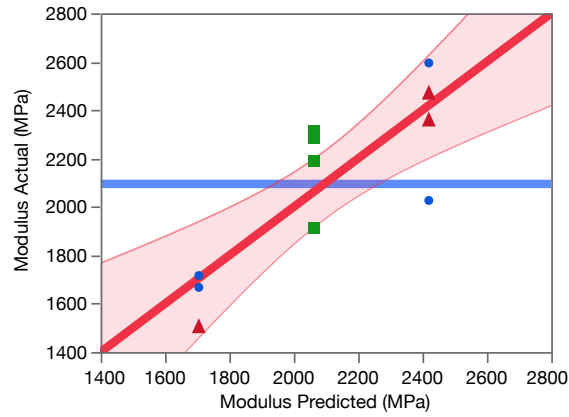
Predictive model

$$\hat{Y}_{modulus} = 2062.28 - 357.34 \times \left(\frac{LH - 0.2}{0.1} \right)$$

Summary of Fit

R-Square	Adjusted R-Square	Root Mean Square Error	Mean of Response
0.698	0.664	206.038	2094.765

Actual by Predicted Plot



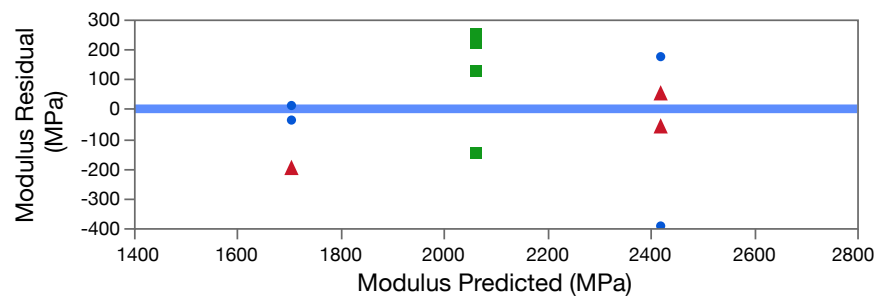
Analysis of Variance

Source	df	Sum of square	Mean Square	F-Ratio	Prob > F
Regression	1	882256.9	882257	20.7825	0.0014
Residual	9	382066.4	42452		
Total	10	1264323.2			

Lack of Fit

Source	df	Sum of square	Mean Square	F-Ratio	Prob > F
Lack of fit	1	80122.5	80122.5	2.1228	0.1832
Pure error	8	301943.9	37743		
Total error	9	382066.4			

Residual by Predicted Plot and Normality of Residuals



Anderson-Darling	
A2	Prob > A2
0.183	0.892

Modelling Crystallinity

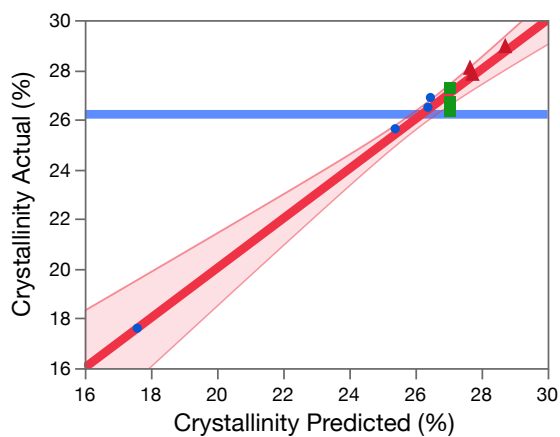
Predictive model

$$\hat{Y}_{crystallinity} = 27.07 + 3.1 \times \left(\frac{T - 390}{20} \right) - 1.93 \times \left(\frac{PS - 40}{20} \right) + 1.97 \times \left(\frac{LH - 0.2}{0.1} \right) - 2.46 \times \left(\frac{WT - 18}{7} \right)$$

Summary of Fit

R-Square	Adjusted R-Square	Root Mean Square Error	Mean of Response
0.983	0.972	0.503	26.208

Actual by Predicted Plot



Analysis of Variance

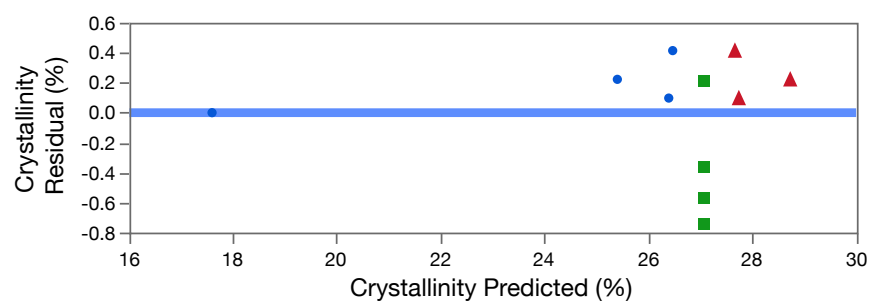
Source	df	Sum of square	Mean Square	F-Ratio	Prob > F
Regression	4	88.602	22.151	87.665	<.00001

Residual	6	1.516	0.253
Total	10	90.118	

Lack of Fit

Source	df	Sum of square	Mean Square	F-Ratio	Prob > F
Lack of fit	3	1.000	0.333	1.938	0.3
Pure error	3	0.516	0.172		
Total error	6	1.516			

Residual by Predicted Plot and Normality of Residuals



Anderson-Darling	
A2	Prob > A2
0.654	0.069

1. C. Basgul, T. Yu, D. W. MacDonald, R. Siskey, M. Marcolongo and S. M. Kurtz, *Journal of the Mechanical Behavior of Biomedical Materials*, 2020, **102**, 103455.
2. M. Luo, X. Tian, W. Zhu and D. Li, *Journal of Materials Research*, 2018, **33**, 1632-1641.
3. P. Han, A. Tofangchi, S. Zhang, A. Desphande and K. Hsu, *Procedia Manufacturing*, 2020, **48**, 737-742.
4. M. Luo, X. Tian, J. Shang, W. Zhu, D. Li and Y. Qin, *Composites Part A: Applied Science and Manufacturing*, 2019, **121**, 130-138.
5. S. Berretta, R. Davies, Y. T. Shyng, Y. Wang and O. Ghita, *Polymer Testing*, 2017, **63**, 251-262.
6. M. F. Arif, S. Kumar, K. M. Varadarajan and W. J. Cantwell, *Materials & Design*, 2018, **146**, 249-259.
7. Q. Li, W. Zhao, Y. Li, W. Yang and G. Wang, *Polymers*, 2019, **11**.
8. P. Consul, A. Chaplin, N. Tagscherer, S. Zaremba and K. Drechsler, *Polymer International*, 2020, **n/a**.